

**Tropical Biogeomorphic Seagrass Landscapes for Coastal Protection  
Persistence and Wave Attenuation During Major Storms Events**

James, R.K.; Lynch, A.; Herman, P.M.J.; van Katwijk, M.M.; van Tussenbroek, B.I.; Dijkstra, H.A.; van Westen, R. M.; van der Boog, C.G.; Klees, R.; Pietrzak, J.D.

**DOI**

[10.1007/s10021-020-00519-2](https://doi.org/10.1007/s10021-020-00519-2)

**Publication date**

2021

**Document Version**

Final published version

**Published in**

Ecosystems

**Citation (APA)**

James, R. K., Lynch, A., Herman, P. M. J., van Katwijk, M. M., van Tussenbroek, B. I., Dijkstra, H. A., van Westen, R. M., van der Boog, C. G., Klees, R., Pietrzak, J. D., Slobbe, C., & Bouma, T. J. (2021). Tropical Biogeomorphic Seagrass Landscapes for Coastal Protection: Persistence and Wave Attenuation During Major Storms Events. *Ecosystems*, 24, 301-318. <https://doi.org/10.1007/s10021-020-00519-2>

**Important note**

To cite this publication, please use the final published version (if applicable).  
Please check the document version above.


**Copyright**

Other than for strictly personal use, it is not permitted to download, forward or distribute the text or part of it, without the consent of the author(s) and/or copyright holder(s), unless the work is under an open content license such as Creative Commons.

**Takedown policy**

Please contact us and provide details if you believe this document breaches copyrights.  
We will remove access to the work immediately and investigate your claim.

# Tropical Biogeomorphic Seagrass Landscapes for Coastal Protection: Persistence and Wave Attenuation During Major Storms Events

R. K. James,<sup>1,2\*</sup>  A. Lynch,<sup>3</sup> P. M. J. Herman,<sup>4</sup> M. M. van Katwijk,<sup>5</sup> B. I. van Tussenbroek,<sup>6</sup> H. A. Dijkstra,<sup>7</sup> R. M. van Westen,<sup>7</sup> C. G. van der Boog,<sup>4</sup> R. Klees,<sup>8</sup> J. D. Pietrzak,<sup>4</sup> C. Slobbe,<sup>8</sup> and T. J. Bouma<sup>1,9</sup>

<sup>1</sup>Department of Estuarine and Delta Systems, NIOZ Royal Netherlands Institute for Sea Research and Utrecht University, Korringaweg 7, 4401 NT Yerseke, The Netherlands; <sup>2</sup>Groningen Institute for Evolutionary Life Sciences, University of Groningen, Groningen, The Netherlands; <sup>3</sup>Department of Environmental Sciences, Wageningen University & Research, Droevendaalsesteeg 4, 6708 PB Wageningen, The Netherlands; <sup>4</sup>Department of Hydraulic Engineering, Delft University of Technology, Stevinweg 1, 2628 CN Delft, The Netherlands; <sup>5</sup>Department of Environmental Science, Institute for Water and Wetland Research, Faculty of Science, Radboud University Nijmegen, Heyendaalseweg 135, 6525 Nijmegen, The Netherlands; <sup>6</sup>Institute of Ocean Sciences and Limnology, Universidad Nacional Autónoma de México, Puerto Morelos, Mexico; <sup>7</sup>Institute for Marine and Atmospheric Research Utrecht, Department of Physics, Utrecht University, Princetonplein 5, 3584 CC Utrecht, The Netherlands; <sup>8</sup>Department of Geoscience and Remote Sensing, Delft University of Technology, Stevinweg 1, 2628 CN Delft, The Netherlands; <sup>9</sup>Department of Physical Geography, Faculty of Geosciences, Utrecht University, P.O. Box 80115, 3508 TC Utrecht, The Netherlands

## ABSTRACT

The intensity of major storm events generated within the Atlantic Basin is projected to rise with the warming of the oceans, which is likely to exacerbate coastal erosion. Nature-based flood defence has been proposed as a sustainable and effective solution to protect coastlines. However, the ability of natural ecosystems to withstand major storms like tropical hurricanes has yet to be thoroughly tested. Seagrass meadows both stabilise sediment and attenuate waves, providing effective coastal protection services for sandy beaches. To examine the tolerance of

Caribbean seagrass meadows to extreme storm events, and to investigate the extent of protection they deliver to beaches, we employed a combination of field surveys, biomechanical measurements and wave modelling simulations. Field surveys of seagrass meadows before and after a direct hit by the category 5 Hurricane Irma documented that established seagrass meadows of *Thalassia testudinum* remained unaltered after the extreme storm event. The flexible leaves and thalli of seagrass and calcifying macroalgae inhabiting the meadows were shown to sustain the wave forces that they are likely to experience during hurricanes. In addition, the seagrass canopy and the complex biogeomorphic landscape built by the seagrass meadows combine to significantly dissipate extreme wave forces, ensuring that erosion is minimised within sandy beach foreshores. The persistence of the Caribbean seagrass meadows and their coastal protection services during extreme storm events ensures that a stable coastal ecosystem and beach foreshore is maintained in tropical regions.

Received 17 January 2020; accepted 27 May 2020;  
published online 15 June 2020

**Electronic supplementary material:** The online version of this article (<https://doi.org/10.1007/s10021-020-00519-2>) contains supplementary material, which is available to authorized users.

**Authors' Contribution** RKJ, AL, PMJH and TJB conceived and designed the study. RKJ and AL performed the research and analysed the data. RKJ wrote the manuscript with contribution from all authors. PMJH and TJB supervised the project and provided critical feedback.

\*Corresponding author; e-mail: Rebecca.james@nioz.nl

**Key words:** Seagrass ecology; Tropical ecosystems; Natural disturbance; *Thalassia*; Cyclone; Hurricane.

## HIGHLIGHTS

- Caribbean seagrass meadows are tolerant of hurricanes.
- Seagrass biogeomorphic landscapes effectively dissipate extreme wave forces.
- Coastal protection services of seagrass meadows ensure a stable ecosystem.

## INTRODUCTION

The frequency of extreme tropical storm events (Cat. 4 & 5 hurricanes) within the North Atlantic is projected to increase with rising sea surface temperatures (Webster and others 2005; Bender and others 2010; Knutson and others 2010, 2013). Enhanced storm activity occurs when the atmosphere becomes destabilised, as a result of the additional energy provided by the warmer sea surface (Smith and others 2010). Between 1996 and 2005, the estimated hurricane frequency within the Atlantic basin was 40–70% above the long-term mean activity since 1950 (Saunders and Lea 2008). Although a lack of historical records makes it uncertain whether this increase in frequency is due to warmer sea surface temperatures from global warming or due to the natural multi-decadal variability observed within the North Atlantic (Lighthill and others 1994; Klotzbach and Gray 2008; Knutson and others 2013), it is clear that the frequency of more extreme hurricane events is increasing within the Atlantic-Caribbean region (Saunders and Lea 2008). Ensuring that tropical coastlines can resist major storms, including hurricanes, is vital for the continued existence of communities living within these regions. Nature-based flood defence has been proposed as a sustainable and effective solution to protect coastlines (Temmerman and others 2013; Morris and others 2018; James and others 2019); however, their ability to withstand major storms like tropical hurricanes has yet to be thoroughly tested.

Caribbean coastal ecosystems are characterised by fringing coral reefs that act as surf breaks (Ferrario and others 2014) and create a sheltered environment behind them. These sheltered regions

fill in with sand, creating lagoons and bays where seagrass can flourish (Saunders and others 2014). Seagrass meadows and coral reefs are interconnected, both biologically (Nagelkerken and van der Velde 2003; Unsworth and others 2008) and physically (Gillis and others 2014, 2017). In addition to being important for biodiversity and fisheries, coral reefs and seagrass meadows provide important coastal protection services (Bouma and others 2014; Ondiviela and others 2014; Saunders and others 2014; Paul 2018; James and others 2019). Coral reefs are a first line of defence, reducing the size of waves entering the bays and lagoons (Saunders and others 2014). Seagrass meadows form a second line of defence, reducing the size of waves reaching the beaches, and thereby reducing beach erosion (Ondiviela and others 2014; James and others 2019). This protective value of seagrass originates both directly from the vegetation's properties as well as from the biogeomorphic bathymetry the seagrass builds.

The flexible leaves of the seagrasses attenuate currents and waves (Bouma and others 2005; Bradley and Houser 2009; Paul and Amos 2011; Hansen and Reidenbach 2012), thereby enhancing the settlement of sediment and inhibiting erosion (Scoffin 1970; Koch and Gust 1999; Koch and others 2006; Hendriks and others 2008, 2010; Peralta and others 2008; Potouroglou and others 2017). Seagrass meadows further stabilise the captured sediment via their dense rhizome-root mat (Christianen and others 2013). Overall, this results in biogeomorphic landscapes, where sediment is captured and stabilised within the beach foreshore (James and others 2019). A complex bathymetry of raised seagrass meadows and cliffs can form where seagrass have continued to capture and retain sediment for long periods (see photo in Figure 2E). Waves get refracted around the topography, and shoaling occurs as the waves propagate into the shallower regions (Paul and Amos 2011). This dispersion of the waves reduces the orbital flow velocity and thereby dissipates the wave energy reaching the shoreline. The attenuation of waves and currents by the seagrass leaves, the capture and stabilisation of sediment, and the resulting creation of a complex bathymetry, together provide a crucial coastal protection service to tropical beaches (Hendriks and others 2010; Christianen and others 2013; James and others 2019).

Major tropical storms and hurricanes produce extreme hydrodynamic forces. The powerful winds generate large waves and strong currents, while storm surges raise the water level, enabling bigger

waves to reach the shoreline (Rodríguez and others 1994). Seagrass and calcifying algae can be uprooted when sediment erodes around the roots and rhizoids (Ball and others 1967; Preen and others 1995; Fourqurean and Rutten 2004), while massive defoliation can occur as the leaves and thalli of the seagrass and algae break from the extreme drag forces of the waves (Pérez and Galindo 2000). Movement of large quantities of sediment can also drastically alter the bathymetry (Ball and others 1967; Rodríguez and others 1994). Studies that have examined the direct effects of extreme storms on seagrass meadows show variable responses, with some meadows displaying limited damage (Ball and others 1967; Steward and others 2006; Anton and others 2009; van Tussenbroek and others 2014), others having a mixed and often species-specific response (Ball and others 1967; Whitfield and others 2002; Fourqurean and Rutten 2004; Cruz-Palacios and Van Tussenbroek 2005), whereas some meadows have been extensively damaged (Rodríguez and others 1994; Preen and others 1995).

A direct response to hurricane forces was observed within seagrass meadows in the Florida Keys after a category 2 hurricane passed in 1998. *Syringodium filiforme* coverage was reduced by 19%, whereas the strong, deep root network of *Thalassia testudinum* allowed it to persist through the extreme hydrodynamic conditions, only experiencing a 3% loss in the leaf biomass (Fourqurean and Rutten 2004). In the Mexican Caribbean, category 4 hurricane Wilma (which lasted 72 h) caused sediment to be deposited along a 5–10-m-wide coastal fringe extending along a 20-km stretch of the coastline, which suffocated seagrass communities (van Tussenbroek, Unpubl. Data, van Tussenbroek and others 2008, 2014). Outside of the Atlantic hurricane region, extreme waves and currents from a category 2 storm in Queensland, Australia, caused seagrass meadows of shallow-rooted *Halophila* spp. to be uprooted from shallow areas (Preen and others 1995). More damaging, however, were the persistent river plumes that limited light for an extended period causing massive seagrass dieback (Preen and others 1995).

Whereas many studies have examined the response of seagrass meadows to hurricanes, none have yet questioned if biogeomorphic seagrass landscapes continue to provide their vital coastal protection services during and following such extreme storm events. Hydrodynamic measurements within the coastal zone during extreme storms are limited (Silva-Casarín and others 2009), with the unpredictability of hurricanes making it difficult to

set up equipment in the right location at the right time and existing equipment is often overwhelmed. This lack of data limits our ability to understand the vulnerability or resistance of coastal ecosystems to extreme storm events. Morphodynamic wave models allow the incorporation of multiple processes, including geodynamics, hydrodynamics, and ecological parameters (Roelvink and others 2009; Ruiz-Martínez and others 2015; Gracia and others 2016; van Rooijen and others 2016). With measurements taken under normal, calm conditions, such comprehensive models can be used to explore the extreme forces that occur during a storm (Roelvink and others 2009; Gracia and others 2016). One of these models is the morphodynamic wave model XBeach (Roelvink and others 2009). With this model, one can study the propagation of extreme hydrodynamic forces over a known coral reef and seagrass ecosystem, while also distinguishing the relative contribution to wave dissipation from vegetation and bathymetry, respectively.

In 2017, the Eastern Caribbean experienced one of its most active and destructive storm seasons since 1970 (Klotzbach and Bell 2017). The category 5 Hurricane Irma caused major devastation on Saint Martin, an island in the Leeward chain of the Caribbean, when it made direct landfall in September of that year. This was closely followed by tropical storm-force winds from Hurricane Jose and subsequently the Category 5 Hurricane Maria passing just south of the island. To examine the response of the seagrass communities, and the influence of the seagrass biogeomorphic landscape on wave propagation during storm events, we (1) evaluated the effect of the intense hurricane season of 2017 on three seagrass meadows in differing hydrodynamic settings at Saint Martin, comparing community surveys and bathymetry before and after the storm season, (2) measured biomechanical properties of the above-ground biomass of dominant seagrass and calcifying macroalgae to assess the physical thresholds of the meadows, and (3) evaluated the dissipative potential of the meadows during the hurricane using the morphodynamic wave model, XBeach, forced with in situ wave measurements taken during calm conditions and configured with the bathymetry of one of the sites. Using XBeach, we systematically assessed the contribution of the seagrass canopy and the biogeomorphic landscape-structures formed by the seagrass meadow. With this research, we aim to enhance current understanding of how Caribbean seagrass meadows tolerate extreme hydrodynamic conditions during these extreme storm events, and to what extent they can continue to provide

important coastal protection services to the beaches they front.

## METHODS

### Site Description

Between October 2015 and March 2016, a monitoring campaign was conducted at three sites on the Eastern coastline of Saint Martin, Caribbean, located within the Leeward island chain (Figure 1). The three neighbouring sites were selected because they exhibited contrasting hydrodynamic regimes: wave-sheltered (Baie de L'Embouchure), wave-exposed (Orient Bay) and unidirectional flow (Islets de L'embouchure). A fringing coral reef extends along the eastern edge of all three sites, sheltering the sites from the largest waves that come directly from the Atlantic Ocean. A peninsula provides a wave-sheltered environment at the site within Baie de L'Embouchure, and the positioning of two islets create an area with strong unidirectional flow at the site at Islets de L'embouchure

(Figure 1). Extensive seagrass meadows of *Thalassia testudinum* and *Syringodium filiforme*, interspersed with calcifying macroalgae from the Halimedaceae and Udoteaceae family, are present at all sites.

September 2017 was one of the most active and destructive hurricane seasons in the Leeward Islands in recorded history (van Dijken 2011), with the eye of Category 5 Hurricane Irma passing directly over Saint Martin, followed a week later by Category 5 Hurricane Maria passing 200 miles south of the island. Local tidal gauges were non-functional during the storms, but hydrodynamic models estimate that at its peak, Hurricane Irma generated a sea surface height anomaly of 0.8 m and significant wave heights of up to 10 m in the region offshore of Saint Martin (Candy 2017; Kuznetsova and others 2019). Six months after Hurricane Irma and Maria, in March 2018, the three study sites were revisited and community surveys and depth profiles along pre-existing transects were repeated to examine whether the strong hurricane season had left any long-lasting effects on the seagrass ecosystems.

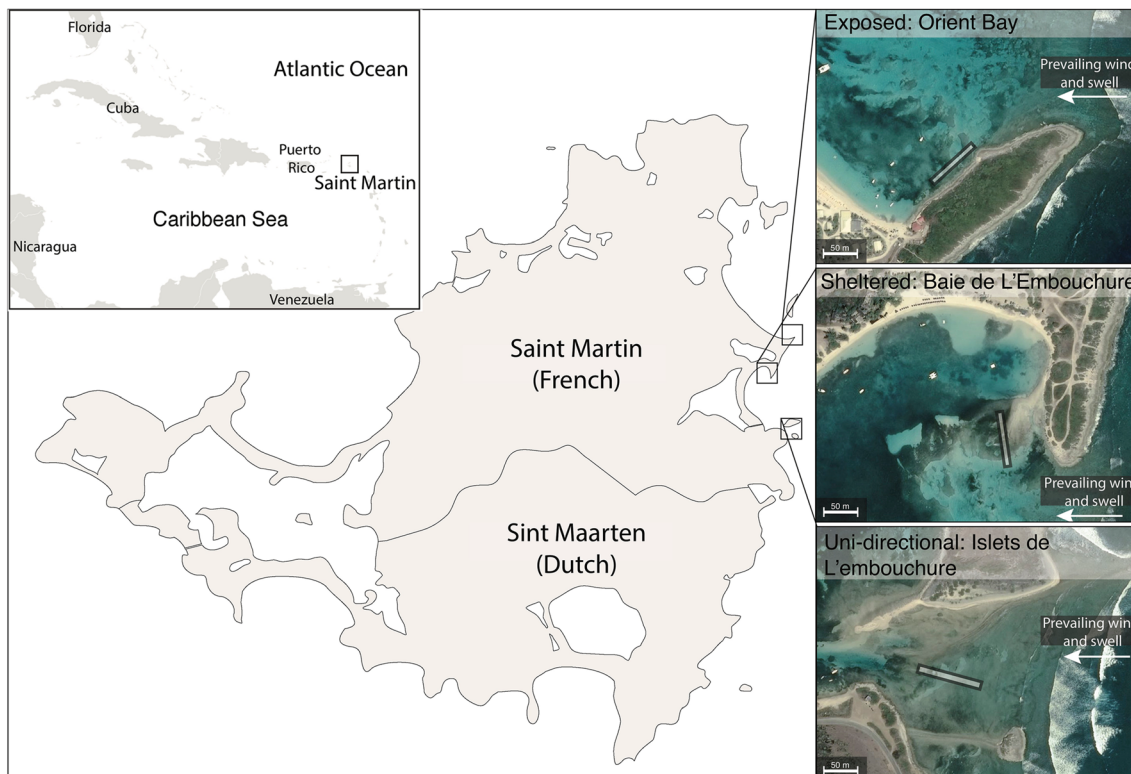


**Figure 1.** Map of the Caribbean island of Saint Martin, displaying the location of the three study sites with contrasting hydrodynamic regimes (exposed, sheltered and unidirectional) on the eastern coast of the island. Transects (white shaded area) were established at the study sites, and were used for the community surveys and other site measurements, before and after the hurricane Irma in 2017. Satellite images obtained from IGN (2019).

## Site Measurements

Saint Martin has a tidal range of less than 30 cm, and all measurements were conducted in the sub-tidal zone in areas shallower than 2 m. Fixed transects measuring 90 m long and 2 m wide were established at least 20–30 m away from the shoreline and extended across the main area of the seagrass meadow (Figure 1).

**Sediment** Triplicate sediment samples were collected in 50-ml sampling containers from each site, both within the centre of the seagrass meadow and adjacent to the meadow in an unvegetated patch to assess the sediment grain size distribution. Sediment samples were freeze-dried and sieved through a 1-mm sieve. Sediment larger than 1 mm was weighed, while the remaining sediment grain size distribution was measured by laser diffraction on a Malvern Mastersizer 2000 (McCave and others 1986). The size of coral rubble pieces that exist in large quantities between the coral reef and the offshore boundary of the seagrass meadow was manually measured. A 30 × 30 cm quadrat was haphazardly placed within the area of coral rubble, and the diameter of pieces on the surface was measured with a ruler.

**Hydrodynamic Forcing** Hydrodynamic forcing at each site was measured on six randomly chosen days from September to December 2015 with typical average wind conditions. Five self-logging pressure sensors (Wave gauge: OSSI-10-003C, Ocean Sensor Systems, Coral Springs, USA; accuracy ± 0.05% FS, resolution 0.0033% FS) were placed along fixed transects: three within the main seagrass meadow, one in an unvegetated patch in front of the meadow and one near the bay entrance 20 m seaward of the transect. The gauges were placed at a height of 0.1 m above the seafloor, and recorded pressure at 5 Hz in 7-minute bursts every 15 min. In total, 100–150 bursts were recorded at each gauge deployment location. Spectral analysis was performed on the pressure time series to obtain wave parameters, such as significant wave height and mean wave period.

**Community Surveys** Community surveys were conducted at each of the three sites (Figure 1) along the 90 m transects in October 2015 and March 2018. Sixty quadrats (0.3 × 0.3 m) were placed along the transects at predetermined random distances. A new set of random sampling positions were chosen for each new community survey. Percentage cover of the taxa present in each quadrat was estimated by trained researchers. Photographs were taken at each quadrat position, to verify the estimated cover. The depth at each

quadrat was measured and visually wave-averaged, giving an accuracy of ± 0.2 m. As the quadrat positions differed between survey years, the depth measurements were not conducted at the exact same points, but were within 0.5 m from each other.

For further analysis, species groups were formed that distinguish the main functional groups at the study sites. Calcifying algae (*Halimeda incrustata*, *Halimeda monile*, *Penicillus capitatus* and *Udotea flabellum*) were grouped together, while the two dominant seagrass species (*T. testudinum* and *S. filiforme*) were kept separate. The two seagrass species represent different successional levels in the community, with *T. testudinum* being a late successional seagrass species, which typically succeeds the colonising species, *S. filiforme* (Williams 1990).

## Morphodynamic Wave Model

XBeach (v1.23, Deltares; Roelvink and others 2009) was used to examine wave propagation over a fringing coral reef and seagrass meadow up to a sandy beach in both calm and hurricane conditions. The sheltered site in Baie de L'Embouchure was used as a case-study (Figure 2). Three scenarios were run for each hydrodynamic forcing to examine the influence of the seagrass canopy and biogeomorphic bathymetry on the wave propagation within the bay. The scenarios were: (1) a smoothed transect that represents a scenario with no biogeomorphic landscape (Figure 2A), (2) a defoliated meadow consisting of the biogeomorphic bathymetry of the seagrass meadow but without the seagrass vegetation (Figure 2B), and (3) a full seagrass meadow with the biogeomorphic bathymetry and seagrass blades (Figure 2C).

**Model Setup** XBeach is a depth-averaged, process-based numerical model that simulates the hydrodynamic processes of short and long wave transformation and propagation across near-shore environments. Numerical simulations were performed with XBeach configured in a one-dimensional mode, along a cross-shore transect one grid cell wide. The 'surfbeat' mode was used, which was shown by van Rooijen and others (2016) to accurately predict wave reduction by vegetation without detailed calibration, and is recommended when the focus is on swash zone processes rather than time-averaged currents and setup. Simulations were run for 10 h of wave attack and 40 h of morphodynamics, with an average hydrodynamic time step of 0.008 s. The 40-hour period was approximately the duration of the peak hydrodynamic impact of Hurricane Irma on Saint Martin on

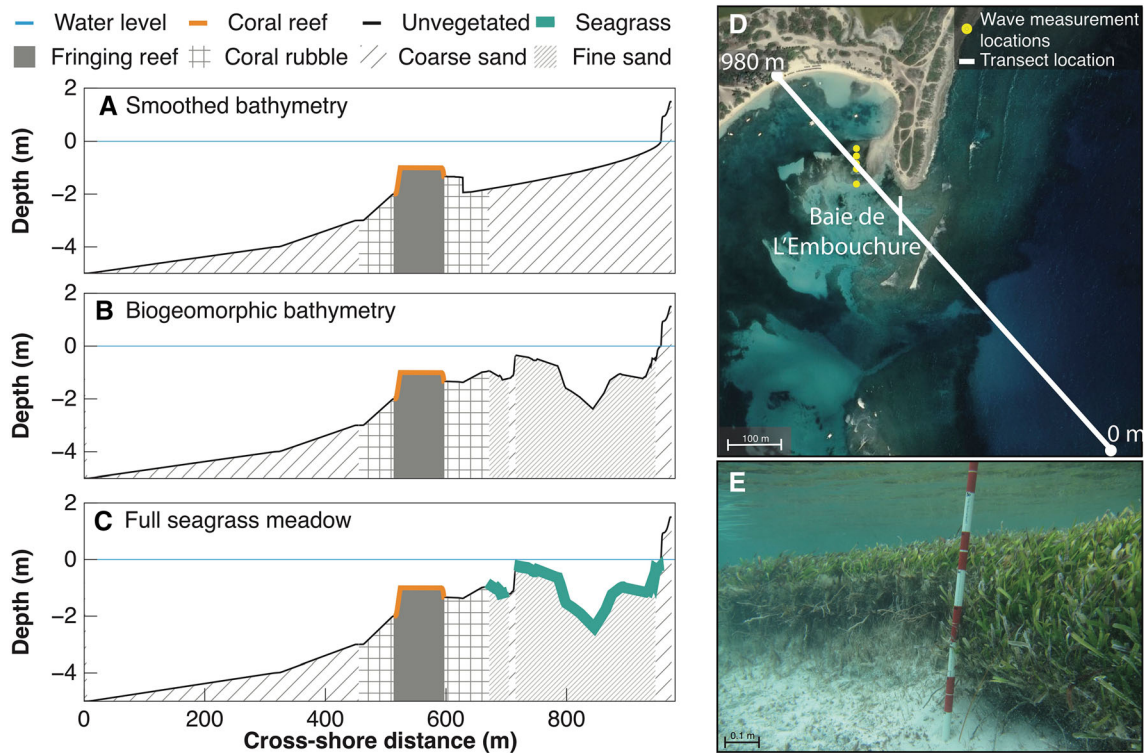


**Figure 2.** Transects of the three scenarios used within the XBeach simulations: smoothed bathymetry (**A**), biogeomorphic bathymetry (**B**) and the present-day scenario with the complete seagrass meadow (**C**). The different grain sizes are indicated as coarse sand (wide diagonal line pattern), coral rubble (cross-hatch pattern), fine sand (fine diagonal line pattern) and carbonate reef (dark grey shading). The orange portion of the depth profile indicates the location of the coral reef and the green shading indicates the seagrass meadow. Satellite image (**D**) shows the position of the transect within Baie de L'Embouchure (white line) and position of the wave measurements (yellow circles). This transect passed over a large raised ( $\sim 0.4$  m) seagrass meadow that is photographed in (**E**).

September 6, 2017. All used model parameters can be found in Suppl. Table 1. For a more extensive model description and formulations of XBeach, we refer to Roelvink and others (2009).

*Transect Setting* The transect which forms the model domain was drawn from Baie de L'Embouchure, across a prominent raised seagrass meadow and the fringing coral reef out to approximately 1 km from shore (Figure 2D). This transect was positioned to capture the typical cross-shore depth profile, while also coinciding with the locations of the wave measurements and community surveys conducted in 2015 and 2018. In 2016, the bathymetry of the study area was measured using dGPS with a Trimble® R8 Rover and base station (Trimble Inc, Sunnyvale, USA; accuracy  $\pm 5$  mm). Reefnet® Sensus Ultra pressure sensors (Reefnet Inc, Ontario, Canada; accuracy  $\pm 30$  cm) were deployed within the bay at two locations for 2 months to determine the average sea level within the bay, and depth measurements were corrected to give the depth at the average sea level. A

bathymetry map was created by interpolation of the measured depths onto an irregular grid using Delft3D pre-processing tools RGFRID and QUICKIN (Deltares 2017), from which the transect profile was extracted. The smoothed transect represented an idealised beach foreshore with no seagrass biogeomorphic landscape and was generated by linearly interpolating a bottom profile from the entrance of Galion Bay (cross-shore distance = 230 m) up to the shoreline, starting at a depth of 2 m, which was the deepest measurement along the natural transect (Figure 2A).

A variable resolution grid was designed to maximise the resolution in particular areas of interest while minimising computational demands. The grid had a resolution of approximately 1.5 m at the offshore boundary, 0.5 m across the coral reef and 0.15 m from the reef to the shoreline. Three sediment fractions are defined along the transect (coral rubble, bare sand, and sand within seagrass meadow), corresponding to their cross-shore location and presence or absence of seagrasses (Figure 2).

The sediment sizes were determined from the sediment grain size measurements taken at the study site, as detailed in the site measurements, and are reported in Suppl. Table 1.

*Vegetation Parameters* Short-wave dissipation by vegetation is implemented in XBeach as a drag force, calculated as a function of the local wave height and the characteristics of vegetation; height above the seafloor, leaf diameter, a bulk drag coefficient ( $C_D$ ), and density (van Rooijen and others 2016). The effect of vegetation on wave propagation is included within XBeach, by implementing formulations that take into account vegetation-induced sea-swell wave attenuation, infragravity wave attenuation, mean flow reduction, and mean water level effects (van Rooijen and others 2016). Vegetation is modelled as rigid cylinders that exert a force on the fluid, as described by Morison and others (1950). The use of rigid cylinders ignores the swaying motion of flexible vegetation, but for a certain range of conditions, and once the correct deflected height and bulk drag coefficient is chosen, it has been shown that flexible vegetation acts similarly to rigid plants (Dijkstra and Uittenbogaard 2010). Although the canopy of dominant *T. testudinum* is up to 0.3 m tall, the deflected height is approximately 0.03 m, as measured in the bending experiments described above. This deflected height of 0.03 m and a blade width of 0.01 m (measured during the biomechanical testing) were used as the *T. testudinum* parameters in the XBeach simulations (Suppl. Table 1).

The bulk drag coefficient ( $C_D$ ) is an expression for the dissipation of wave energy and force exerted by the fluid on the entire seagrass meadow (Mendez and Losada 2004; Bradley and Houser 2009; Sánchez-González and others 2011; Pinsky and others 2013). This differs from the drag coefficient which classically examines just a single plant. It is difficult to determine the  $C_D$  for flexible vegetation as it cannot be directly measured in the field and varies greatly in the natural situation (Mendez and Losada 2004; Bradley and Houser 2009; Ozeren and others 2014). The  $C_D$  is therefore generally estimated or used for calibration in hydrodynamic models (Baptist and others 2007). Pinsky and others (2013) calculated the  $C_D$  of seagrass meadows using published data and displayed that seagrass meadows can exhibit  $C_D$  ranging from 0.46 up to 4.87. Given the large range of potential  $C_D$  for seagrass meadows, we calibrated the  $C_D$  against our wave measurements from the site. To acknowledge

the large variations in  $C_D$  values, we have also included a wave propagation model simulation for  $C_D = 0.4$  within Suppl. 2, which demonstrates the sensitivity of the wave propagation model to this parameter.

Distribution of seagrass along the transect was inferred from the community surveys as described above, and from satellite imagery. The shoot density of well-developed *T. testudinum* meadows was calculated from  $0.3 \times 0.3$  m quadrats placed at random within the study area, giving a density of 1000 shoots  $m^{-2}$ .

*Boundary Forcings* For calm conditions, the wave model was forced on the offshore boundary with a wave-energy spectrum derived from the NOAA WAVEWATCH III® model (Tolman 2009). Average significant wave height, direction and period were extracted in the region offshore of Saint Martin. Simulated propagation of waves in calm conditions into Baie de L'Embouchure is validated against the wave gauge measurements that have been described above.

For the hurricane simulations, offshore wave parameters and the storm surge level during Hurricane Irma were obtained from Caribbean Watch (Candy 2017), which infers ocean conditions in the Caribbean sea from the Mercator Ocean reanalysis dataset. No measured data from within the bay were available for verification of the wave propagation during the storm, nor were data available from the tidal gauge at Marigot, on the western side of Saint Martin, to validate the storm surge at the coast. We can therefore not be certain that our simulations directly reflect the conditions within the bay during Hurricane Irma; however, the depth at the offshore boundary was max. 5 m, which is too shallow to support larger waves than what were simulated in this study. We are, therefore, confident that the simulations represent an extreme tropical storm event for the region studied.

*Analysis* Fit functions were fit to the simulated  $H_{rms}$  significant wave heights across the first 150 m of the seagrass meadow (from 672 to 882 m in the cross-shore), where the majority of the wave dampening by the seagrass meadow occurred. The equations from these fits were used to assess the different rates of wave decay between the three bathymetric scenarios. When wave decay was present, an exponential function was fit ( $y = ae^{bx}$ ), otherwise a linear fit was used. 95% confidence intervals for the simulated  $H_{rms}$  and  $U_{rms}$  were calculated from the 37 time steps, after data were tested for normality and passed this assumption.



## Biomechanical Properties of Vegetation

*Vegetation Collection* Fifteen shoots of the seagrass *T. testudinum*, and thalli of the calcifying macroalgae *H. monile*, *H. incrassata* and *P. capitatus* were collected from Saint Martin in April 2016. They were left overnight in seawater bubbled with air, then wrapped in moist paper towels and transported by plane to NIOZ-Yerseke in The Netherlands (total travel time was 12 h). The shoots and thalli were placed in a heated seawater tank set to 25°C, bubbled continuously with air with 12 h d<sup>-1</sup> light (550 µmol m<sup>-2</sup> s<sup>-1</sup> Photosynthetic Active Radiation; PAR). The seagrass and calcifying macroalgae were left for 24 h to recover from the transport.

*Drag Forces and Bending Angles* Drag forces experienced by the seagrass *T. testudinum*, and the calcifying macroalgae *H. monile*, *H. incrassata* and *P. capitatus* were measured following the methods of Bouma and others (2005). Drag was considered as the force exerted on the base of the shoot or thallus, and was measured at flow velocities in 0.1 m s<sup>-1</sup> increments from 0 to 0.5 m s<sup>-1</sup> in a unidirectional racetrack flume. Drag measurements were replicated at least 15 times for each species, with each replicate being conducted on a new individual. The roots and rhizomes were removed and the individuals were attached at the base of their stem/thallus to a force transducer developed by WLDelft Hydraulics (Delft, The Netherlands; for details see Bouma and others 2005). Special care was made when attaching the individuals to ensure that there was no sideways movement of the individual in the clamp. The widest surface of the individuals was positioned perpendicular to the current, the natural positioning of the individuals in situ. Voltage readings from the force transducer were logged with Delft-Measure (Deltares) at 10 Hz and measured over a one-minute period at each velocity. The mean voltage readings were calculated and used for further analysis. Calibration was done in analogy to Stewart (2004), and voltage readings were converted to Newtons (N).

Photographs were taken of the individuals at each flow velocity to calculate the bending angles. Using Image J (Schneider and others 2012), the bending angle from the base of the stem to the most distal part of the thallus was measured. The change in bending angle from the starting position was calculated and used for further data analysis. Additionally, the total height of *T. testudinum* when bending at a flow velocity of 0.3 m s<sup>-1</sup> was measured from the photos for use in the XBeach simulations.

*Leaf/Thallus Force to Tear* The absolute force required to break the leaf/thallus of the seagrass/calcifying macroalgae was measured with a tensometer (Instron® model 3342). Measurements were conducted following methods by La Nafie and others (2012) and De los Santos and others (2016). Seagrass blades were cut at the junction between the sheath and the blade, while 50 mm portions of the secondary branches of *Halimeda* spp., and the stalk portion of *P. capitatus* were used. These portions were individually clamped into Instron® screw grips (Cat. No. 2710-102), with the mountings spaced 20 mm apart. The leaves and thalli were stretched at a rate of 5 mm min<sup>-1</sup>, and the extension (\*s; mm) and the force (*F*, N) were recorded every 0.1 s until the blades/thalli broke. The maximum tension force that the blades/thalli could bear before breaking was recorded and defined as the absolute force to tear. The absolute force to tear is used as a proxy for the force required to defoliate the seagrass meadow.

## RESULTS

### Before and After Community Surveys with Depth Profiles

Between October 2015 and March 2018, there were relatively minor changes in the depth profiles and seagrass cover at the three sites, even though the intense hurricane season of 2017 had occurred a few months prior to the final surveys (Figure 3).

At the sheltered site, *Thalassia testudinum* had the densest cover at a mean of 81 ± 8.7% (± 95% CI, *n* = 55) in Oct. 2015 (Figure 3C) and 82 ± 4.9% (*n* = 60) in March 2018 (Figure 3B). The sheltered site is characterised by a raised seagrass meadow with a steep cliff up to 1 m high (see photo in Figure 2E) and a shallow area of about 0.3 m (Figure 3A). Between 2015 and 2018, there was an observed shallowing of the seagrass meadow at the transect distances 0–10 m and 47–80 m. *T. testudinum* and *Syringodium filiforme* grew over an unvegetated patch at 35–45 m along the transect between 2015 and 2018, resulting in a more uniform coverage of *T. testudinum* across the site (Figure 3B).

At the exposed site, *T. testudinum* had a sparser and patchier coverage compared to the sheltered and unidirectional flow sites, with a mean site coverage of 39 ± 8.3% (± 95% CI, *n* = 56) in 2015 (Figure 3F) and 34 ± 7.1% (± 95% CI, *n* = 60) in the 2018 survey (Figure 3E). Both *T. testudinum* and *S. filiforme* were lost at 25–30 m and 42–45 m along the transect; however *T. testudinum* did in-

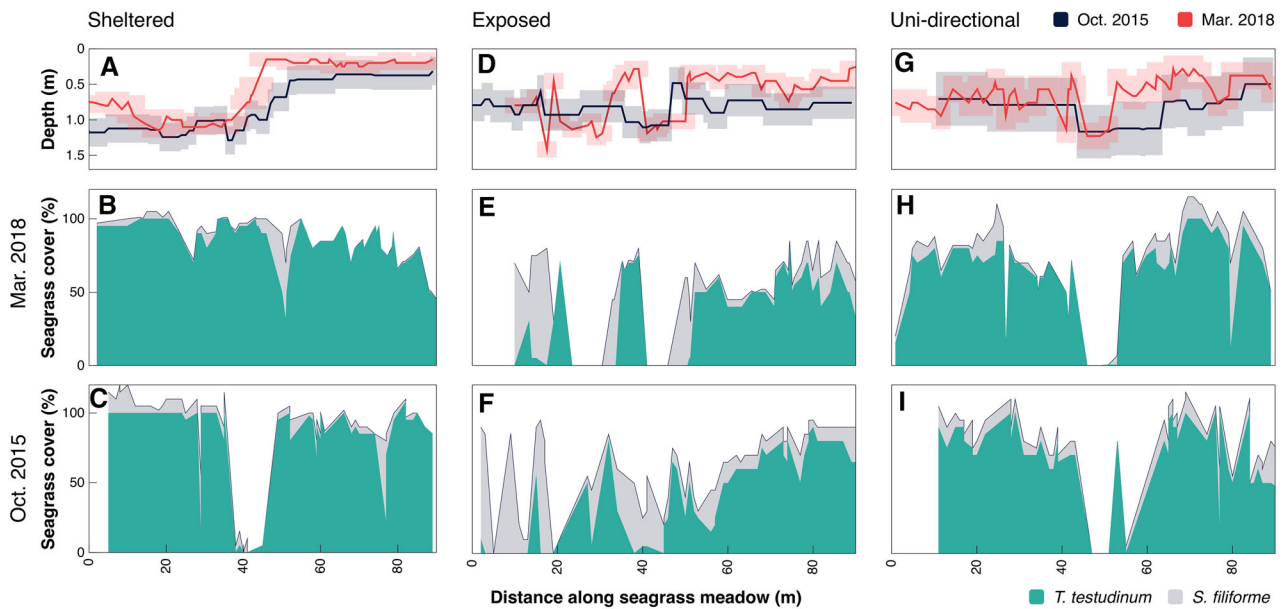


**Figure 3.** Depth profiles and seagrass cover at the three study sites with contrasting hydrodynamic regimes (sheltered, exposed and unidirectional), before (October 2015) and after (March 2018) the intense hurricane season in September 2017. Depth was measured at each quadrat in 2015 (black) and 2018 (red line), lighter shading around the line represents the measurement uncertainty from approximate wave-averaging. Seagrass cover was estimated for the two dominant seagrass species, *Thalassia testudinum* (green shading) and *Syringodium filiforme* (light grey shading). The transects extended from the seaward edge of the meadow (transect distance = 0 m) towards the landward edge (transect distance = 90 m).

crease in cover at 20 and 55 m. The bed-level increased in large areas where the seagrass remained between 2015 and 2018 (Figure 3D).

There was little change in the vegetated community at the unidirectional flow site (Figure 3H, I). *T. testudinum* had a mean cover of 65% both in 2015 (95% CI = 7.8%,  $n = 60$ ; Figure 3I) and 2018 (95% CI = 6.6%,  $n = 60$ ; Figure 3H). The only significant change in the bed-level at the unidirectional flow site occurred between 50 and 60 m, where the seagrass meadow extended across an unvegetated region resulting in this region becoming shallower (Figure 3G).

### Calibration of XBeach

Wave measurements along the established transect at the sheltered site displayed how the waves dissipate as they travel across the seagrass meadow (Figure 4A). At the seaward edge of the seagrass meadow, the wave height ( $H_{rms}$ ) was measured as  $0.18 \pm 0.005$  m (95% CI,  $n = 116$ ; Figure 4). By the time the waves had propagated 64 meters over the biogeomorphic seagrass landscape, the wave height was reduced to  $0.05 \pm 0.003$  m (95% CI,  $n = 116$ ; Figure 4). There was no significant correlation of the measured wave properties with the average wind strength or wind direction of the

measurement day, indicating that the primary driver of the wave forces is the Atlantic swell entering the bay from the East.

A bulk drag coefficient of  $C_D = 4$  produced the best agreement between the measured and simulated significant wave heights within the present-day seagrass simulation. Only the unvegetated area at the seaward edge of the raised meadow (cross-shore distance: 708 m) showed a discrepancy between measured and simulated values (Figure 4A), with the measured waves being on average 0.08 m smaller than those calculated in XBeach. This observed discrepancy between the measured and simulated waves may be due to the transect used for the simulations being positioned 4–45 m away from where the wave measurements were conducted (Figure 2D) and also due to our model simulations not including wave reflection. As the trend between the modelled and measured waves was similar and overlapped with each other, we considered the simulations to give a good estimate of the interaction between the biogeomorphic landscape of the seagrass meadow and the wave propagation within the studied situation. A  $C_D$  of 0.4 has also been included within Suppl. 2 to display the sensitivity of the wave propagation model to the  $C_D$ .

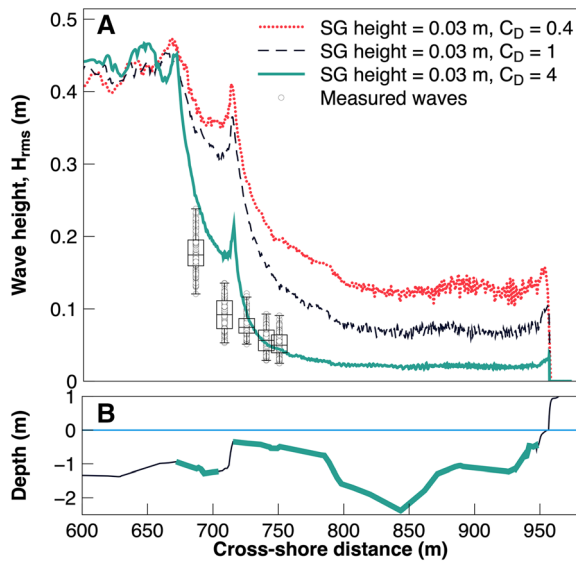


**Figure 4.** Calibration of the bulk drag coefficient of the seagrass meadow for XBeach simulations. Wave heights ( $H_{rms}$ ) are displayed from the model runs with a seagrass deflection height of 0.03 m and different bulk drag coefficients (**A**):  $C_D = 0.4$  (blue dotted line),  $C_D = 1$  (black dashed line), and  $C_D = 4$  (green solid line). The model runs were validated against the waves measured at Baie de L'Embouchure (open circles with box plots), to determine an appropriate  $C_D$  for use in further simulations. The depth profile of the cross-shore transect (**B**) is shown with green shading indicating presence of seagrass.

### Modelled Wave Dissipation by Biogeomorphic Seagrass Landscapes in Calm Conditions

The incoming waves from the Atlantic Ocean were modelled to reach the seaward edge of the coral reef (cross-shore distance = 513 m) with a depth-averaged orbital velocity ( $U_{rms}$ ) of  $0.63 \pm 0.06 \text{ m s}^{-1}$  (95% CI,  $n = 73$ ) and wave height ( $H_{rms}$ ) of  $0.84 \pm 0.07 \text{ m}$  (95% CI,  $n = 73$ ; Figure 5B). Wave breaking over the shallow coral reef resulted in a reduced orbital velocity of  $0.36 \pm 0.02 \text{ m s}^{-1}$  (95% CI,  $n = 73$ ; Figure 5A) at the landward edge of the reef (cross-shore distance = 598 m). This was associated with a 51% reduction in the wave height, so that waves entering Baie de L'Embouchure had a  $H_{rms}$  of  $0.41 \pm 0.01 \text{ m}$  (95% CI,  $n = 73$ ; Figure 5B).

With no biogeomorphic landscape in the model, and only a steady incline up to the shoreline (smoothed bathymetry scenario), there was no wave dissipation within the bay (Figure 6A), and the waves reached the beach slope (cross-shore distance = 930 m) with a rms height of

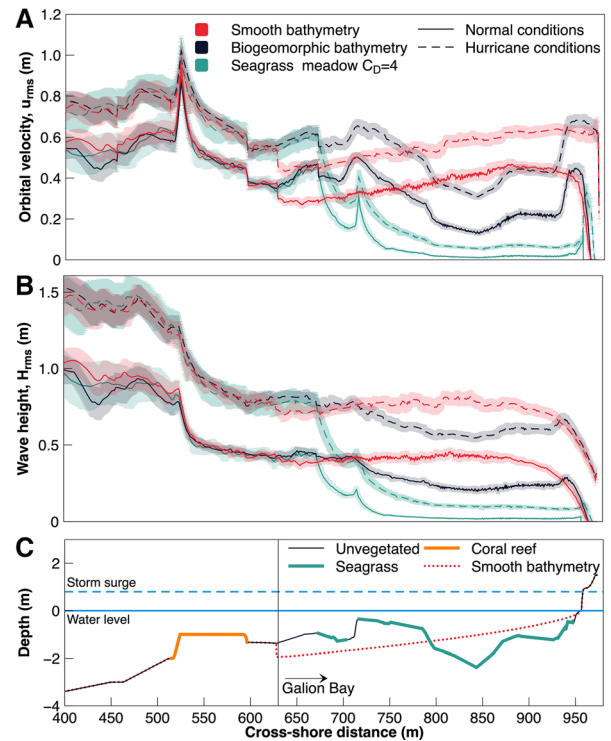


**Figure 5.** Simulated depth-averaged orbital velocity ( $U_{rms}$ ; **A**) and mean wave height ( $H_{rms}$ ; **B**) along the cross-shore transect (**C**) under calm conditions (solid lines) and hurricane conditions (dashed lines). Simulations were run for the three scenarios: smoothed bathymetry (red lines), biogeomorphic bathymetry (black line), and the natural seagrass meadow (green line). Lines represent the time-averaged mean ( $n = 73$ ) from each model run, and the shaded area around the lines indicates the 95% confidence intervals. **C** shows the depth profile over the cross-shore transect, with coral reef (orange) and seagrass meadow (green). The dotted red line indicates the depth profile used for the smoothed transect scenario. The water level (solid blue line) was increased by a storm surge of 0.8 m (dashed blue line) during Hurricane Irma.

$0.30 \pm 0.003 \text{ m}$  (95% CI,  $n = 73$ ; Figure 6A) before breaking. These larger waves are calculated to create an orbital velocity at the beach slope of  $0.43 \pm 0.004 \text{ m s}^{-1}$  (95% CI,  $n = 73$ ; Figure 5A).

With the addition of the biogeomorphic bathymetry within the model, the wave height exponentially decayed within the first 150 m of the biogeomorphic landscape with a decay coefficient of  $-0.005 \text{ m}^{-1}$  (Figure 6A). This dissipation resulted in waves reaching the beach slope that were 20% smaller in height and which imposed an orbital velocity that was 50% lower than the smoothed bathymetry simulation (Figures 5A, 6A). In the natural situation, with the addition of the seagrass canopy on the complex biogeomorphic

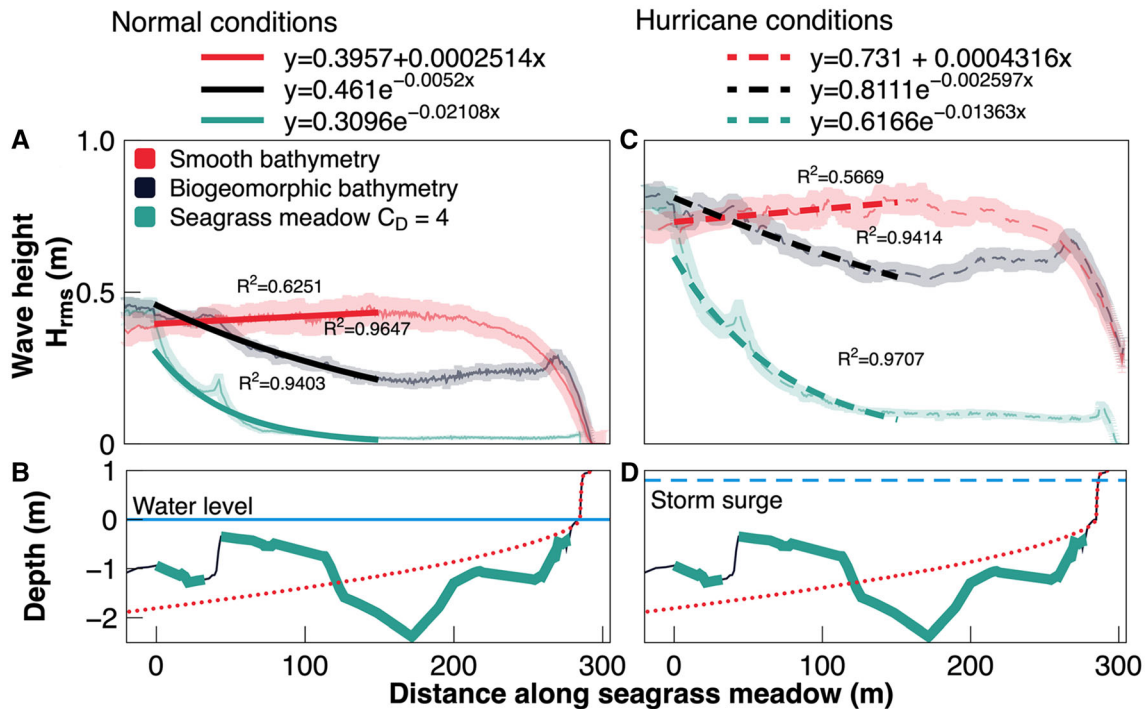


Figure 6. The modelled wave height ( $H_{rms}$ ) of waves as they propagate across the location of the seagrass meadow within Baie de L'Embouchure under calm conditions (A) and hurricane conditions (C). Trend lines (bold lines) are fitted to the three scenarios: smoothed bathymetry (red line; linear fit), biogeomorphic bathymetry (black line; exponential fit), the natural seagrass meadow (green line; exponential fit). The depth profiles B, D display the transect used for the smoothed bathymetry scenario (red dotted line) and the natural biogeomorphic bathymetry scenarios (solid black line), with the green shading indicating where seagrass is present. Lines represent the time-averaged mean ( $n = 73$ ), and the shaded area directly around the lines indicates the 95% confidence intervals.

bathymetry, the exponential decay coefficient increased to  $-0.02 \text{ m}^{-1}$  indicating that the presence of a seagrass canopy induces wave dissipation at a rate 4 times greater than that of a biogeomorphic landscape alone. Once the waves reached the start of the beach slope (cross-shore distance = 930 m), the wave height had reduced to  $0.017 \pm 0.003 \text{ m}$  (95% CI,  $n = 73$ ; Figure 6A) and there was an orbital velocity of  $0.016 \pm 0.003 \text{ m s}^{-1}$  (95% CI,  $n = 73$ ; Figure 5A), a 95% reduction in the wave forces compared to the smoothed bathymetry scenario (Figures 5A, 6A).

### Modelled Effect of Hurricanes on the Wave Dissipation by Biogeomorphic Landscapes

The same trends are observed in the hurricane-like scenarios, when there was a storm surge of 0.8 m and the non-breaking wave height at the seaward edge of the fringing coral reef was 51% greater compared to calm conditions (Figure 5B). The coral reef still provided a strong dissipative effect; however, the deeper waters and larger waves at the

offshore boundary resulted in non-breaking waves with a  $H_{rms}$  of  $0.78 \pm 0.01 \text{ m}$  (95% CI,  $n = 73$ ; Figure 5B) passing the coral reef and entering the bay. An  $U_{rms}$  of  $0.55 \pm 0.004 \text{ m s}^{-1}$  (95% CI,  $n = 73$ ; Figure 5A) was calculated at the landward edge of the coral reef.

Without the seagrass meadow and biogeomorphic bathymetry in hurricane conditions, no wave dissipation occurred within the bay and the non-breaking waves were estimated to reach the beach slope with a 56% greater  $H_{rms}$  of  $0.68 \pm 0.03 \text{ m}$  (95% CI,  $n = 73$ ; Figure 6B), and causing a 33% greater  $U_{rms}$  of  $0.64 \pm 0.03 \text{ m s}^{-1}$  (95% CI,  $n = 73$ ; Figure 6C, D) compared to calm conditions.

The deeper waters from the 0.8 m storm surge resulted in the bathymetry within the bay having less effect on the wave dissipation (Figure 6). The complex biogeomorphic bathymetry did still cause the wave height to exponentially decay with a coefficient of  $-0.003 \text{ m}^{-1}$ ; however, this was 50% less than the same scenario under calm conditions (Figure 6). The wave dissipation by the bathymetry resulted in waves at the beach slope that were 7% smaller with an orbital velocity that was 27%

slower compared with the smooth bathymetry scenario during hurricane-like conditions (Figure 6B).

The seagrass canopy had a similar dissipative effect as under calm conditions, with the seagrass meadow dissipating the wave height with an exponential decay coefficient of  $-0.014 \text{ m}^{-1}$  (Figure 6B). The non-breaking waves under hurricane conditions reached the beach slope with a  $H_{\text{rms}}$  of  $0.08 \pm 0.01 \text{ m}$  (95% CI,  $n = 73$ ; Figure 6B) and an  $U_{\text{rms}}$  of  $0.06 \pm 0.01 \text{ m s}^{-1}$  (95% CI,  $n = 73$ ) after being dissipated by the seagrass meadow and biogeomorphic bathymetry. The presence of the biogeomorphic bathymetry and seagrass meadow in hurricane-like conditions caused a 90% reduction in the wave height and orbital velocity compared to the smoothed bathymetry scenario (Figure 6B).

### Biomechanical Properties of Vegetation

Biomechanical measurements of the different vegetation species under increasing unidirectional flow speeds displayed how the breaking force of the above-ground biomass far exceeds the drag forces that the individuals would experience in situ (Figure 7C). At a unidirectional flow speed of  $0.5 \text{ m s}^{-1}$  (that is, slightly lower than the peak orbital velocity during hurricanes; Figure 5) the leaves of the seagrass *T. testudinum* bent to a low angle

(Figure 7B), and therefore, only experienced a drag force of  $0.05 \pm 0.01 \text{ N}$  (95% CI,  $n = 16$ ; Figure 7A). This drag force is two orders of magnitude lower than the  $9.66 \pm 1.05 \text{ N}$  (95% CI,  $n = 24$ ) of tension force required to tear the leaves of a healthy *T. testudinum* plant (Figure 7C). The calcifying algae *H. incrassata* are made up of many segments that break apart at a tension force of  $1.78 \pm 0.73 \text{ N}$  (95% CI,  $n = 17$ ; Figure 7C). *H. incrassata* bent low to the ground when exposed to flow (Figure 7B), resulting in it experiencing very little drag under strong unidirectional flow (Figure 7A). *H. monile* grows in large clumps and remains mostly upright. Of all species measured, it experienced the strongest drag forces. Nevertheless, the measured drag force of  $0.12 \pm 0.02 \text{ N}$  (95% CI,  $n = 24$ ; Figure 7A) imposed on thalli of *H. monile* at  $0.5 \text{ m s}^{-1}$ , was well below the tension force required to break its segmented thallus ( $2.00 \pm 0.46 \text{ N}$ , 95% CI,  $n = 26$ ; Figure 7C). The heavily calcified stalk of *P. capitatus* required a tension force of  $22.15 \pm 2.52 \text{ N}$  (95% CI,  $n = 23$ ; Figure 7C) to break. The thin stalk and spherical ‘brush head’ morphology of *P. capitatus* experienced little drag ( $0.07 \pm 0.01 \text{ N}$ , 95% CI,  $n = 24$ ; Figure 7A), even though the thick calcified stalk bent only up to an angle of  $11 \pm 3.4^\circ$  (95% CI,  $n = 24$ ; Figure 7B) at  $0.5 \text{ m s}^{-1}$ .

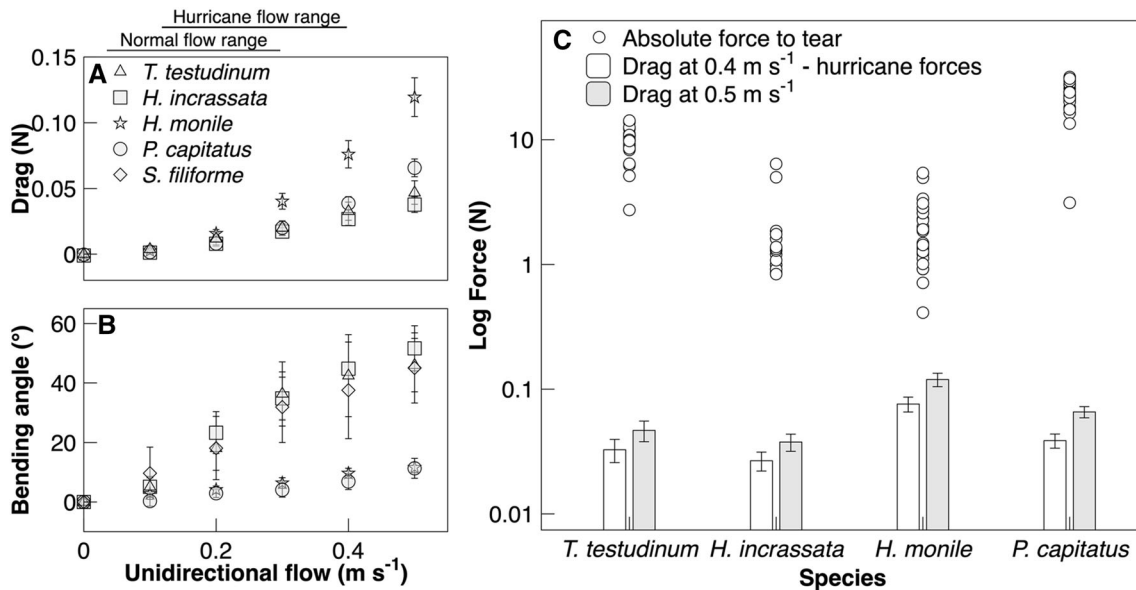


Figure 7. The drag (A) and degree of bending (B) that the leaves of *Thalassia testudinum* (triangles), *Syringodium filiforme* (diamonds), and thalli of *Halimeda incrassata* (squares), *Halimeda monile* (stars) and *Penicillus capitatus* (circles) experience under increasing flow velocities. The flow range under calm and storm conditions is indicated above. The log force (N) required to tear the leaves and thalli of the seagrass and algae is displayed in (C, circles), with the log drag forces (N) experienced at  $0.4 \text{ m s}^{-1}$  (white bars), and at  $0.5 \text{ m s}^{-1}$  (grey bars). Points and bars represent means  $\pm$  95% CI.

## DISCUSSION

Offshore waves during Hurricane Irma were up to 10 m in height (Candy 2017; Kuznetsova and others 2019). These large waves in combination with the storm surge resulted in non-breaking waves entering Baie de L'Embouchure that were 90% larger compared to calm conditions. Even with these extreme hydrodynamic forces, there was very little change in the bathymetry or community structure within the *Thalassia testudinum*-dominated seagrass meadows. Not only were the seagrass meadows tolerant of the extreme storm conditions, our observations and the wave propagation model display how the seagrass meadows continue to provide important coastal protection services during extreme hydrodynamic events. Both the seagrass canopy and the complex biogeomorphic bathymetry created by the raised seagrass beds significantly dissipate the waves within a shallow bay under both calm and hurricane-like conditions, reducing the wave forces that reach the shoreline. In addition, the ability of the seagrass meadows to withstand the extreme hydrodynamic forces ensures that the seafloor integrity is maintained. The robustness of the coastal protection services provided by seagrass meadows to extreme hydrodynamic events highlights the importance of a seagrass-vegetated foreshore to protect beaches within tropical coastal zones, especially as the frequency of extreme storms is expected to increase.

### Tolerance of Caribbean Seagrass Meadows

Only the most exposed site (Orient Bay) exhibited a reduction in the cover of *T. testudinum*, with the loss of a small area of seagrass near the seaward edge of the meadow. Both the unidirectional flow and sheltered sites remained in a stable state, and actually expanded into bare areas over the survey period, displaying the general succession of the seagrass community (Williams 1990). Given that the final surveys were conducted 6 months after the hurricane events on Saint Martin, there may have been changes to the seagrass meadow that were not observed. However, considering there were no significant changes to the seagrass meadows after 6 months demonstrates that the intense hurricane season in the Caribbean 2017 had no long-lasting impact on the local seagrass meadows.

The minimal response of the studied seagrass meadows to strong hurricane events is comparable to what has been reported previously in other *T. testudinum*-dominated seagrass meadows (Four-

qurean and Rutten 2004; Byron and Heck 2006; Anton and others 2009; van Tussenbroek and others 2014). The tolerance of native Caribbean seagrass meadows to the extreme hydrodynamic forces caused by hurricanes is likely to be an evolutionary adaptation (Botero and others 2015).

### Traits to Withstand Extreme Hydrodynamic Forces

Major hurricanes of category 4 and 5 occur at an average rate of 2.4 events per year within the Caribbean (Bender and others 2010), with islands in the northern leeward chain (in the vicinity of Saint Martin) experiencing category 3–5 hurricanes approximately once every 10 years (van Dijken 2011). For a species to persist and become dominant in Caribbean tropical ecosystems, they need traits which allow them to tolerate the extreme but recurrent storm events. The biomechanical measurements display how the flexible but strong leaves of *T. testudinum* bend low over the sediment surface, thereby reducing the drag force which they are subjected to, even in flows surpassing the hurricane level. The flexibility and strength of the healthy leaves and thalli of the seagrass and algae ensures that extreme hydrodynamic forces are unlikely to cause extensive defoliation of the seagrass meadows.

The mechanical analyses were conducted with unidirectional flow conditions, which do not capture the swaying motion of the flexible vegetation that occurs under orbital wave motion. This swaying motion can cause extra forces of whip-like accelerations (Gaylord and Denny 1997; Gaylord and others 2008), and therefore, our biomechanical measurements may underestimate the forces that the seagrass and calcifying macroalgae experience under wave forces. However, as the seagrass and calcifying algae are relatively short (< 30 cm) (Gaylord and Denny 1997; Bouma and others 2005) and the extra forces from swaying have been shown to only be important when the ratio between wave velocity and current speed is large (Gosselin 2019; Lei and Nepf 2019), the impact of swaying motion is expected to be limited. Given that the tension force required to break the leaves and thalli of the vegetation was an order of magnitude greater than the drag forces simulated during a hurricane, breakage of healthy leaves and thalli of seagrass and calcifying macroalgae is expected to be unlikely during hurricanes. Additionally, the robust and deep root-rhizome mat of mature *T. testudinum* meadows ensures that dis-

lodgment is unlikely during strong hydrodynamic events.

The persistence of the *T. testudinum* root-rhizome mat ensures maintenance of a stable sediment surface, which is beneficial for the seagrass itself (Williams 1990; van Tussenbroek and others 2008; Christianen and others 2014; Suykerbuyk and others 2016), and also for other benthic organisms inhabiting the meadow. The upright thalli of the calcifying algae species require forces greater than what a hurricane can produce to break; however, their rhizoid-root system can be prone to dislodgment when in unconsolidated sand (van Tussenbroek and others 2008). These calcifying algae have a network of rhizoids which clump together with the sand, creating a small ball below the sediment surface that keeps them rooted in place (Cruz-Palacios and Van Tussenbroek 2005). When sediment is eroded around this rhizoid-root system, the calcifying algae can become dislodged. The persistence of the *T. testudinum*-dominated meadow, however, provides a stable, consolidated sediment surface, reducing the risk of dislodgement of the calcifying algae and other benthic species inhabiting the seagrass meadows.

### Persistent Coastal Protection Services of Beaches

Wave attenuation by seagrass meadows is well documented (Bouma and others 2005; Bradley and Houser 2009; Paul and Amos 2011); however, there is very little knowledge on the significance of this wave dissipation during extreme hydrodynamic events, such as storms. This study has highlighted the tolerance of the Caribbean's native seagrass meadows to extreme hydrodynamic forces imposed by hurricanes, which ensures that they continue to provide important coastal protection services throughout major storm events.

Our bathymetric surveys display how the continued existence of the seagrass meadow over the two-year survey period protects the seafloor from erosion, and in many instances, resulted in an increase in the bed-level. Additionally, the wave propagation model, based on bathymetry and in situ wave measurements during calm conditions, displays how the combination of the seagrass canopy and the complex biogeomorphic bathymetry effectively dissipates the waves in the shallow bay as they propagate across the meadow, even during extreme storm events. Wave attenuation by the bathymetry is restricted to the areas where there is shallowing. The waves shoal and break where the seabed changes depth, causing a significant reduc-

tion in the wave forces at localised areas. After the waves break; however, further attenuation by the bathymetry is limited due to the waves being adapted to the shallower depth. The extensive and dense seagrass meadow imposes vegetation drag and increases the seabed roughness over a large area of the domain. Because the seagrass meadow is so extensive, the waves are attenuated over a large area of the foreshore, contributing to a significant reduction in the hydrodynamic forces.

It must be noted that the level of wave attenuation by vegetation is dependent on the height of the seagrass relative to the local water depth (Fonseca and Cahalan 1992). As our study site is shallow (0.3–2 m depth), the 0.2 m tall seagrass canopy is very effective at dissipating waves, even with a storm surge of 0.8 m. Storm surges of this magnitude are typical for the Caribbean region due to the steeply sloping shelves around many of the islands (Daniel 1996; Beven and others 2008). The Gulf coast, however, is typified by a gently sloping shelf, which creates much larger storm surges (1.0–8.5 m) during extreme storms (Beven and others 2008). In situations where the seagrass canopy occupies less of the water column, the effectiveness of seagrass at attenuating waves would be reduced (Fonseca and Cahalan 1992; Barbier and others 2008; Ozeren and others 2014). Nevertheless, the reduction in the erodibility of the seafloor by the seagrass meadow in addition to the wave dissipation by the biogeomorphic landscape makes natural seagrass meadows extremely effective at protecting tropical foreshores and shorelines from erosion (James and others 2019).

Without the biogeomorphic bathymetry and the seagrass canopy, the orbital velocity created by waves travelling up the smooth inclining bathymetry increases along the transect and the waves break at the shoreline with a force similar to the waves that first enter the bay (Figure 5). However, within the natural seagrass meadow landscape, waves decay at an exponential rate over the first 150 m of the seagrass meadow, resulting in significantly lower hydrodynamic forces crossing the bay and reaching the shoreline in both calm and hurricane conditions. Smaller and more fragmented meadows are likely to be limited in their dissipative power (Bradley and Houser 2009). It is therefore important to protect and restore meadows of a sufficient size if coastal regions wish to benefit from the effective coastal protection services provided by seagrass meadows.

## Importance of Surrounding Ecosystems

In line with Ferrario and others (2014), the fringing coral reef is modelled to be extremely effective at dissipating waves and thereby in providing a protected environment behind it both during calm and hurricanes conditions (Saunders and others 2014). The rigid coral reefs create a barrier that can be as shallow as 0.5 m deep, thereby providing a natural seawall that filters out the largest waves from entering the bay. Without this fringing reef, the seagrass meadows would be much more vulnerable to erosion, experiencing the full force of the incoming waves from the open ocean (Saunders and others 2014).

Vegetation on the shoreline can also contribute to maintaining the seagrass meadows in a healthy condition. Heavy rainfall is often associated with tropical storm events, which can dramatically increase the run-off from the land. Rainfall run-off can increase the sediment load within the surrounding coastal waters, potentially disrupting the light supply to seagrass meadows (Preen and others 1995) and increasing the nutrient loads into the coastal ecosystems (McGlathery and others 2007). Mangroves and shoreline vegetation are extremely effective at trapping and filtering the run-off from the terrestrial environment (Valiela and Cole 2002; Gillis and others 2014), and are thereby important for buffering the seagrass meadows from any potentially damaging run-off, particularly during storm events. Although we have no direct measurements, mangrove forests surrounding estuarine areas adjacent to Baie de L'Embouchure likely help to minimise the sediment load within the bay, particularly during and after extreme storm events. Sediment resuspension caused by the extreme hydrodynamic forces during storms can also induce high turbidity (Ward and others 1984; Preen and others 1995). The coarse calcareous sediment found within many tropical coastal regions, including Baie de L'Embouchure, however, quickly sinks out of the water column, and typically does not increase turbidity for long periods (Shields 1936; Adams and others 2016).

## CONCLUSION

Hurricanes produce extreme hydrodynamic conditions that can cause extensive damage to tropical marine ecosystems. Due to the recurrent nature of hurricanes within the Caribbean, native species have had to adapt to the associated extreme hydrodynamic forces in order to survive (Botero and others 2015). We showed that well-established

*T. testudinum*-dominated native Caribbean seagrass meadows and their coastal protection services persist during major tropical storms and hurricanes. Leaves of *T. testudinum* and thalli of dominant calcifying macroalgae sustain any wave forces they are likely to experience as a result of hurricane activity. Revisited transects were almost unaltered after the multiple hurricanes of 2017, and a model using bathymetry and wave measurements showed that waves in a shallow bay were greatly attenuated by the seagrass canopy. By stabilising the sediment and dissipating waves, seagrass meadows minimise erosion of sandy beach foreshores. These coastal protection services are also beneficial for other benthic species and the seagrass species themselves, as the risk of dislodgment is decreased. The tolerance of native Caribbean seagrass meadows and the effectiveness of their coastal protection services during calm and extreme hydrodynamic conditions are both essential for their persistence but also provide a vital ecosystem service by maintaining a stable coastal ecosystem. This tolerance of seagrass coastal protection services to hurricanes is especially important as the frequency of major storm events is projected to increase with the warming oceans.

## ACKNOWLEDGEMENTS

Thank you to Vera van Berlo and Margot van Malenstein for their help in conducting the original community surveys. This work was primarily funded by the Nederlandse Organisatie voor Wetenschappelijk (NWO) 'Caribbean Research: a Multidisciplinary Approach' grant, which was awarded to the SCENES Project (Grant Number 858.14.063). Permits for the work in St Martin were obtained from the Reserve Naturelle Saint Martin, and we are grateful for their advice and allowing us to conduct our research there.

## OPEN ACCESS

This article is licensed under a Creative Commons Attribution 4.0 International License, which permits use, sharing, adaptation, distribution and reproduction in any medium or format, as long as you give appropriate credit to the original author(s) and the source, provide a link to the Creative Commons licence, and indicate if changes were made. The images or other third party material in this article are included in the article's Creative Commons licence, unless indicated otherwise in a credit line to the material. If material is not included in the article's Creative Commons licence



and your intended use is not permitted by statutory regulation or exceeds the permitted use, you will need to obtain permission directly from the copyright holder. To view a copy of this licence, visit <http://creativecommons.org/licenses/by/4.0/>.

## DATA AVAILABILITY

All data available at 4TU.Centre for Research Data (<https://researchdata.4tu.nl/>; <https://doi.org/10.4121/uuid:d6b7dd41-fa76-4b81-ada4-ca03167ca382>).

## REFERENCES

- Anton A, Cebrian J, Duarte CM, Heck KL, Goff J. 2009. Low impact of Hurricane Katrina on seagrass community structure and functioning in the northern Gulf of Mexico. *Bull Mar Sci* 85:45–59.
- Ball MM, Shinn EA, Stockman KW. 1967. The geologic effects of Hurricane Donna in South Florida. *Journal* 75:583–97.
- Baptist MJ, Babovic V, Uthurburu JR, Keijzer M, Uittenbogaard RE, Mynett A, Verwey A. 2007. On inducing equations for vegetation resistance. *J Hydraul Res* 45:435–50.
- Barbier EB, Koch EW, Silliman BR, Hacker SD, Wolanski E, Primavera J, Granek EF, Polasky S, Aswani S, Cramer LA, Stoms DM, Kennedy C, Bael D, Kappel CV, Perillo GME, Reed DJ. 2008. Coastal ecosystem—based ecological functions and values. *Science* (80-) 319:321–3.
- Bender MA, Knutson TR, Tuleya RE, Sirutis JJ, Vecchi GA, Garner ST, Held IM. 2010. Modeled impact of anthropogenic warming on the frequency of intense Atlantic hurricanes. *Science* (80-) 327:454–8.
- Beven JL, Avila LA, Blake ES, Brown DP, Franklin JL, Knabb RD, Pasch RJ, Rhome JR, Stewart SR. 2008. Atlantic hurricane season of 2005. Miami, Florida.
- Botero CA, Weissing FJ, Wright J, Rubenstein DR. 2015. Evolutionary tipping points in the capacity to adapt to environmental change. *Proc Natl Acad Sci* 112.
- Bouma TJ, van Belzen J, Balke T, Zhu Z, Airoidi L, Blight AJ, Davies AJ, Galvan C, Hawkins SJ, Hoggart SPG, Lara JL, Losada IJ, Maza M, Ondiviela B, Skov MW, Strain EM, Thompson RC, Yang S, Zanuttigh B, Zhang L, Herman PMJ. 2014. Identifying knowledge gaps hampering application of intertidal habitats in coastal protection: opportunities & steps to take. *Coast Eng* 87:147–57.
- Bouma TJ, De Vries MB, Low E, Peralta G, Táncoz IC, Van De Koppel J, Herman PMJ. 2005. Trade-offs related to ecosystem engineering: a case study on stiffness of emerging macrophytes. *Ecology* 86:2187–99.
- Bradley K, Houser C. 2009. Relative velocity of seagrass blades: implications for wave attenuation in low-energy environments. *J Geophys Res Earth Surf* 114:1–13.
- Byron D, Heck KL. 2006. Hurricane effects on seagrasses along Alabama's Gulf Coast. *Estuar Coasts*.
- Candy AS. 2017. Caribbean watch. <https://candylib.org/caribbeanwatch/>. Accessed 20 July 2009.
- Christianen MJA, van Belzen J, Herman PMJ, van Katwijk MM, Lamers LPM, van Leent PJM, Bouma TJ. 2013. Low-canopy seagrass beds still provide important coastal protection services. *PLoS One* 8.
- Christianen MJA, Herman PMJ, Bouma TJ, Lamers LPM, van Katwijk MM, van der Heide T, Mumby PJ, Silliman BR, Engelhard SL, van de Kerk M, Kiswara W, van de Koppel J. 2014. Habitat collapse due to overgrazing threatens turtle conservation in marine protected areas. *Proc R Soc B Biol Sci* 281:20132890–20132890. <http://rspb.royalsocietypublishing.org/cgi/doi/10.1098/rspb.2013.2890>.
- Cruz-Palacios V, Van Tussenbroek BI. 2005. Simulation of hurricane-like disturbances on a Caribbean seagrass bed. *J Exp Mar Bio Ecol* 324:44–60.
- Daniel P. 1996. A real-time system for forecasting hurricane storm surges over the French Antilles. *Coast Estuar Stud* 51:146–56.
- Deltares. 2017. Delft3D-Flow. <https://oss.deltares.nl/web/delft3d>.
- De los Santos CB, Onoda Y, Vergara JJ, Pérez-Lloréns JL, Bouma TJ, La Nafie YA, Cambridge ML, Brun FG. 2016. A comprehensive analysis of mechanical and morphological traits in temperate and tropical seagrass species. *Mar Ecol Prog Ser* 551:81–94.
- Dijkstra JT, Uittenbogaard RE. 2010. Modeling the interaction between flow and highly flexible aquatic vegetation. *Water Resour Res* 46:1–14.
- Ferrario F, Beck MW, Storlazzi CD, Micheli F, Shepard CC, Airoidi L. 2014. The effectiveness of coral reefs for coastal hazard risk reduction and adaptation. *Nat Commun* 5. <http://www.nature.com/doi/10.1038/ncomms4794>.
- Fonseca MS, Cahalan JA. 1992. A preliminary evaluation of wave attenuation by four species of seagrass. *Estuar Coast Shelf Sci* 35:565–76.
- Fourqurean JW, Rutten LM. 2004. The impact of Hurricane Georges on soft-bottom, back reef communities: site- and species-specific effects in south Florida. *Bull Mar Sci* 75:239–57.
- Gaylord B, Denny ME, Koehl MAR. 2008. Flow forces on seaweeds: field evidence for roles of wave impingement and organism inertia. *Biol Bull* 215:295–308.
- Gaylord BP, Denny MW. 1997. Flow and flexibility. *J Exp Biol* 200:3141–64.
- Gillis LG, Bouma TJ, Jones CG, Van Katwijk MM, Nagelkerken I, Jeuken CJL, Herman PMJ, Ziegler AD. 2014. Potential for landscape-scale positive interactions among tropical marine ecosystems. *Mar Ecol Prog Ser* 503:289–303.
- Gillis LG, Jones CG, Ziegler AD, van der Wal D, Breckwoldt A, Bouma TJ. 2017. Opportunities for protecting and restoring tropical coastal ecosystems by utilizing a physical connectivity approach. *Front Mar Sci* 4:374.
- Gosselin FP. 2019. Mechanics of a plant in fluid flow. *J Exp Bot* 70:3533–48.
- Gracia V, García M, Grifoll M, Sánchez-Arcilla A. 2016. Breaching of a barrier under extreme events. The role of morphodynamic simulations. *J Coast Res* 65:951–6.
- Hansen JCR, Reidenbach MA. 2012. Wave and tidally driven flows in eelgrass beds and their effect on sediment suspension. *Mar Ecol Prog Ser* 448:271–87.
- Hendriks IE, Bouma TJ, Morris EP, Duarte CM. 2010. Effects of seagrasses and algae of the Caulerpa family on hydrodynamics and particle-trapping rates. *Mar Biol* 157:473–81.
- Hendriks IE, Sintès T, Bouma TJ, Duarte CM. 2008. Experimental assessment and modeling evaluation of the effects of

- the seagrass *Posidonia oceanica* on flow and particle trapping. *Mar Ecol Prog Ser* 356:163–73.
- IGN. 2019. géoportail. Inst Natl L'Information Géographique For.
- James RK, Silva R, van Tussenbroek BI, Escudero-Castillo M, Mariño-Tapia I, Dijkstra HA, van Westen RM, Pietrzak JD, Candy AS, Katsman CA, van der Boog CG, Riva RE, Slobbe C, Klees R, Stapel J, van der Heide T, van Katwijk MM, Herman PMJ, Bouma TJ. 2019. Maintaining tropical beaches with seagrass and algae: a promising alternative to engineering solutions. *Bioscience* 69:136–42. <https://academic.oup.com/bioscience/advance-article/doi/10.1093/biosci/biy154/5253357>.
- Klotzbach PJ, Bell MM. 2017. Summary of 2017 Atlantic tropical cyclone activity and verification of authors' seasonal and two-week forecasts. Fort Collins, CO.
- Klotzbach PJ, Gray WM. 2008. Multidecadal variability in North Atlantic tropical cyclone activity. *J Clim* 21:3929–35.
- Knutson TR, McBride JL, Chan J, Emanuel K, Holland G, Landsea C, Held I, Kossin JP, Srivastava AK, Sugi M. 2010. Tropical cyclones and climate change. *Nat Geosci* 3:157–63. <http://dx.doi.org/10.1038/NNGEO779%0Ahttp://hdl.handle.net/1721.1/62558>.
- Knutson TR, Sirutis JJ, Vecchi GA, Garner S, Zhao M, Kim HS, Bender M, Tuleya RE, Held IM, Villarini G. 2013. Dynamical downscaling projections of twenty-first-century atlantic hurricane activity: CMIP3 and CMIP5 model-based scenarios. *J Clim* 26:6591–617.
- Koch EW, Ackerman JD, Verduin J, van Keulen M. 2006. Fluid dynamics in seagrass ecology—from molecules to ecosystems. In: Larkum AWD, Orth RJ, Duarte CM, Eds. *Seagrasses: biology, ecology and conservation*. Dordrecht: Springer. p 193–225.
- Koch EW, Gust G. 1999. Water flow in tide and wave dominated beds of the seagrass *Thalassia testudinum*. *Mar Ecol Ser* 184:63–72.
- Kuznetsova A, Baydakov G, Dosaev A, Sergeev D, Troitskaya Y. 2019. Wind waves modeling under hurricane wind conditions. *J Phys Conf Ser* 1163.
- La Nafie Y, de los Santos CB, La Brun FG, van Katwijk MM, Bouma TJ. 2012. Waves and high nutrient loads jointly decrease survival and separately affect morphological and biomechanical properties in the seagrass *Zostera noltii*. *Limnol Oceanogr* 57:1664–72.
- Lei J, Nepf H. 2019. Wave damping by flexible vegetation: connecting individual blade dynamics to the meadow scale. *Coast Eng* 147:138–48. <https://doi.org/10.1016/j.coastaleng.2019.01.008>.
- Lighthill J, Holland G, Gray W, Landsea C, Craig G, Evans J, Kurihara Y, Guard C. 1994. Global climate change and tropical cyclones. *Bull Am Metrol Soc* 75:2147–57.
- McGlathery KJ, Sundbäck K, Anderson IC. 2007. Eutrophication in shallow coastal bays and lagoons: the role of plants in the coastal filter. *Mar Ecol Prog Ser* 348:1–18.
- Mendez FJ, Losada IJ. 2004. An empirical model to estimate the propagation of random breaking and nonbreaking waves over vegetation fields. *Coast Eng* 51:103–18.
- Morison JR, Johnson JW, Schaaf SA. 1950. The force exerted by surface waves on piles. *J Pet Technol* 189:149–54.
- Morris RL, Konlechner TM, Ghisalberti M, Swearer SE. 2018. From grey to green: efficacy of eco-engineering solutions for nature-based coastal defence. *Glob Change Biol* 24:1827–42.
- Nagelkerken I, van der Velde G. 2003. Connectivity between coastal habitats of two oceanic Caribbean islands as inferred from ontogenetic shifts by coral reef fishes. *Gulf Caribb Res* 14:43–59.
- Ondiviela B, Losada IJ, Lara JL, Maza M, Galván C, Bouma TJ, van Belzen J. 2014. The role of seagrasses in coastal protection in a changing climate. *Coast Eng*.
- Ozeren Y, Wren DG, Wu W. 2014. Experimental investigation of wave attenuation through model and live vegetation. *J Waterw Port, Coast Ocean Eng* 140:1–13.
- Paul M. 2018. The protection of sandy shores—Can we afford to ignore the contribution of seagrass? *Mar Pollut Bull* 134:152–9. <https://doi.org/10.1016/j.marpolbul.2017.08.012>.
- Paul M, Amos CL. 2011. Spatial and seasonal variation in wave attenuation over *Zostera noltii*. *J Geophys Res Ocean* 116:1–16.
- Peralta G, Van Duren LA, Morris EP, Bouma TJ. 2008. Consequences of shoot density and stiffness for ecosystem engineering by benthic macrophytes in flow dominated areas: a hydrodynamic flume study. *Mar Ecol Prog Ser* 368:103–15.
- Pérez D, Galindo L. 2000. Efectos de la hiposalinidad en *Thalassia testudinum* (Hydrocharitaceae) del Parque Nacional Morrocoy, Venezuela. *Rev Biol Trop* 48:251–60.
- Pinsky ML, Guannel G, Arkema KK. 2013. Quantifying wave attenuation to inform coastal habitat conservation. *Ecosphere* 4.
- Potouroglou M, Bull JC, Krauss KW, Kennedy HA, Fusi M, Daffonchio D, Mangora MM, Githaiga MN, Diele K, Huxham M. 2017. Measuring the role of seagrasses in regulating sediment surface elevation. *Sci Rep* 1–11. [www.nature.com/scientificreports](http://www.nature.com/scientificreports).
- Preen AR, Lee Long WJ, Coles RG. 1995. Flood and cyclone related loss, and partial recovery, of more than 1000 km<sup>2</sup> of seagrass in Hervey Bay, Queensland, Australia. *Aquat Bot* 52:3–17.
- Rodríguez RW, Webb RMT, Bush DM. 1994. Another look at the impact of Hurricane Hugo on the shelf and coastal resources of Puerto Rico, USA. *J Coast Res* 10:278–96.
- Roelvink D, Reniers AD, van Dongeren AP, van van Thiel de Vries J, McCall R, Lescinski J. 2009. Modelling storm impacts on beaches, dunes and barrier islands. *Coast Eng* 56:1133–52. <https://doi.org/10.1016/j.coastaleng.2009.08.006>.
- Ruiz-Martínez G, Mariño-Tapia I, Mendoza Baldwin EG, Silva Casarín R, Enríquez Ortiz CE. 2015. Identifying coastal defence schemes through morphodynamic numerical simulations along the northern coast of Yucatan, Mexico. *J Coast Res* 651–70.
- Sánchez-González JF, Sánchez-Rojas V, Memos CD. 2011. Wave attenuation due to *Posidonia oceanica* meadows. *J Hydraul Res* 49:503–14.
- Saunders MI, Leon JX, Callaghan DP, Roelfsema CM, Hamylton S, Brown CJ, Baldock T, Golshani A, Phinn SR, Lovelock CE, Hoegh-Guldberg O, Woodroffe CD, Mumby PJ. 2014. Interdependency of tropical marine ecosystems in response to climate change. *Nat Clim Change* 4:1–6. <http://www.nature.com/nclimate/journal/vaop/ncurrent/full/nclimate2274.html?message-global=remove>.
- Saunders MA, Lea AS. 2008. Large contribution of sea surface warming to recent increase in Atlantic hurricane activity. *Nature* 451:557–60.
- Schneider CA, Rasband WS, Eliceiri KW. 2012. NIH Image to ImageJ: 25 years of image analysis. *Nat Methods* 9: 671–75.

- Scoffin TP. 1970. The trapping and binding of subtidal carbonate sediments by marine vegetation in Bimini Lagoon, Bahamas. *J Sediment Petrol* 40:249–73.
- Silva-Casarín R, Mendoza-Baldwin E, Escalante-Mancera E, Mariño-Tapia I, Ruiz-Rentería F. 2009. Wind waves induced by hurricane Wilma in Puerto Morelos, Quintana Roo, Mexico | Oleaje inducido por el huracán Wilma en Puerto Morelos, Quintana Roo, México. *Ing Hidraul en Mex* 24.
- Smith DM, Eade R, Dunstone NJ, Fereday D, Murphy JM, Pohlmann H, Scaife AA. 2010. Skilful multi-year predictions of Atlantic hurricane frequency. *Nat Geosci* 3:846–9. <http://doi.org/10.1038/ngeo1004>.
- Steward JS, Virnstein RW, Lasi MA, Morris LJ, Miller JD, Hall LM, Tweedale WA. 2006. The impacts of the 2004 hurricanes on hydrology, water quality, and seagrass in the Central Indian River Lagoon, Florida. *Estuar Coasts* 29:954–65.
- Stewart HL. 2004. Hydrodynamic consequences of maintaining an upright posture by different magnitudes of stiffness and buoyancy in the tropical alga *Turbinaria ornata*. *J Mar Syst* 49:157–67.
- Suykerbuyk W, Bouma TJ, Govers LL, Giesen K, de Jong DJ, Herman P, Hendriks J, van Katwijk MM. 2016. Surviving in changing seascapes: sediment dynamics as bottleneck for long-term seagrass presence. *Ecosystems* 19:296–310.
- Temmerman S, Meire P, Bouma TJ, Herman PMJ, Ysebaert T, De Vriend HJ. 2013. Ecosystem-based coastal defence in the face of global change. *Nature* 504:79–83. <https://doi.org/10.1038/nature12859>.
- Tolman H. 2009. User manual and system documentation of WAVEWATCH III (tm) version 3.14, Tech. Note 276. <https://github.com/NOAA-EMC/WW3>.
- Unsworth RKF, De León PS, Garrard SL, Jompa J, Smith DJ, Bell JJ. 2008. High connectivity of Indo-Pacific seagrass fish assemblages with mangrove and coral reef habitats. *Mar Ecol Prog Ser*.
- Valiela I, Cole ML. 2002. Comparative evidence that salt marshes and mangroves may protect seagrass meadows from land-derived nitrogen loads. *Ecosystems* 5:92–102.
- van Dijken G. 2011. Caribbean Hurricane Network. <https://stormcarib.com>. Accessed 26 Aug 2019.
- van Rooijen AA, McCall RT, de Thiel de Vries JSM, van Dongeren AR, Reniers AJHM, Roelvink JA. 2016. Modeling the effect of wave-vegetation interaction on wave setup. *J Geophys Res Ocean* 121:4341–59.
- van Tussenbroek BI, Barba Santos MG, van Dijk JK, Sanabria Alcaraz SNM, Téllez Calderón ML. 2008. Selective elimination of rooted plants from a tropical seagrass bed in a back-reef lagoon: a hypothesis tested by Hurricane Wilma (2005). *J Coast Res* 24:278–81.
- van Tussenbroek BI, Cortés J, Collin R, Fonseca AC, Gayle PMH, Guzmán HM, Jácome GE, Juman R, Koltés KH, Oxenford HA, Rodríguez-Ramírez A, Samper-Villarreal J, Smith SR, Tschirky JJ, Weil E. 2014. Caribbean-wide, long-term study of seagrass beds reveals local variations, shifts in community structure and occasional collapse. *PLoS One* 9.
- Ward LG, W MK, Boynton WR. 1984. The influence of waves and seagrass communities on suspended particulates in an estuarine embayment. *Mar Geol*.
- Webster PJ, Holland GJ, Curry JA, Chang H-R. 2005. Changes in tropical cyclone number, duration, and intensity in a warming environment. *Science* (80-) 309:1844–6.
- Whitfield PE, Kenworthy WJ, Hammerstrom KK, Fonseca MS. 2002. The role of a hurricane in the expansion of disturbances initiated by motor vessels on seagrass banks. *J Coast Res SI* 37:86–99.
- Williams SL. 1990. Experimental studies of Caribbean seagrass bed development. *Ecol Monogr* 60:449–69.